A New Method for Assessing the Exploratory Field of View (EFOV)

Enkelejda Tafaj[1], Sebastian Hempel[1], Martin Heister[2], Kathrin Aehling[2], Janko Dietzsch[2], Frank Schaeffel[2], Wolfgang Rosenstiel[1] and Ulrich Schiefer[2]

[1]*Wilhelm-Schickard Institute, Computer Engineering Department, University of Tübingen, Tübingen, Germany*

[2]*Centre for Ophthalmology, Institute for Ophthalmic Research, University of Tübingen, Tübingen, Germany*

Keywords: Exploratory Field of View, Visual Exploration, Visual Field, Ophthalmology, Eye Movements.

Abstract: Intact visual functioning is a crucial prerequisite for driving safely. Visual function tests usually include the assessment of the visual acuity and binocular visual field. Based on these results, persons suffering from some types of visual field defects that affect the central 20 degree region are prohibited from driving, although they may have developed patterns of eye and head movements that allow them to compensate for their visual impairment. We propose a new method to assess the exploratory field of view (EFOV), i.e. the field of view of a subject when eye movements are allowed. With EFOV testing we aim at capturing the visual exploration capability of a subject and thus understand the real impact of visual field defects on activities of daily living and potential compensatory strategies.

1 INTRODUCTION

Visual information accounts for up to 90% of driving related-inputs (Taylor, 1982). The assessment of the visual acuity and visual field are therefore important elements of ability tests in traffic ophthalmology. According to current recommendations, subjects suffering from binocular visual field defects affecting the central 20 degree region are prohibited from driving. Visual field testing, i.e. *perimetry*, consists of measuring the sensitivity of visual perception as a function of location in the visual field (Schiefer et al., 2008). The stimuli are projected onto a homogenous curved background. In *kinetic* perimetry, a stimulus with constant luminance is moved from blind areas almost perpendicularly towards the assumed visual field defect border. The position at which the presented stimulus is detected, represets the border and/or the outer limit of the visual field. *Static* perimetry is mainly performed automatically by computer-driven stimulus presentation. The size and location of a stimulus is kept constant while its luminance varies, usually in a stepwise up- and-down manner. Subjects indicate stimulus perception by pressing a response button. A missing response to a stimulus projection is interpreted as a failure to seeing it (Schiefer et al., 2008).

Although perimetry is a highly standardized psychophysical method, it is yet rather artificial. In everyday but safety critical activities such as driving a car, subjects are usually neither confronted with small, rather dim light stimuli on an homogeneous background nor do they have to refrain from eye and head movements. Instead, conspicuous objects within the visual field induce a shift of the visual attention, eliciting eye and head movements towards the object of interest. These types of movements can also help to - at least partially - compensate for existing visual defects. Several studies, e.g. (Martin et al., 2007), (Hardiess et al., 2010), (Pambakian et al., 2000), (Riley et al., 2007), have been conducted to explore the viewing behavior of persons with advanced visual field defects such as homonymous, where half of the visual field in both eyes is affected. These studies confirmed that persons who have developed a good exploration capability are able, by performing efficient eye and head movements towards their visual field defect, to obtain information from the impaired part of the visual field. Present ability testing does address ocular motility, however only with regard to disclose double vision during smooth pursuit instead of unveiling insufficient saccadic eye movements towards objects of interest.

In this paper we introduce a new method to assess the exploratory field of view (EFOV), i.e. the field of view of a person when eye movements are allowed. During EFOV testing, the subject is encouraged to move his eyes towards the presented stimulus in order to fixate it. EFOV testing can capture the visual

Tafaj E., Hempel S., Heister M., Aehling K., Dietzsch J., Schaeffel F., Rosenstiel W. and Schiefer U..
A New Method for Assessing the Exploratory Field of View (EFOV).
DOI: 10.5220/0004190600050011
In *Proceedings of the International Conference on Health Informatics* (HEALTHINF-2013), pages 5-11
ISBN: 978-989-8565-37-2

exploration capability of a subject and thus reveal the real impact of a visual field defect. Implementation details and exemplary results of the assessment of the exploratory field of view will be presented in the following sections.

2 THE EXPLORATORY FIELD OF VIEW (EFOV) TEST

The Exploratory Field Of View (EFOV) Test is implemented for usage with cupola perimeters such as the Octopus 900 perimeter (HAAG-STREIT Inc., Koeniz, Switzerland) depicted in Figure 1. The perimetric system itself consists of an examination unit, Octopus 900 cupola, and a control unit, Figure 1. The control unit is a notebook computer or a PC that communicates with the examination element via an Ethernet link. For fixation stability, the Octopus perimeters are equipped with a camera directed to the subject's eye. The eye is illuminated with infrared LEDs and then captured by a CMOS camera at an image resolution of $320 \times 240 px$ and a sampling rate of 20Hz.

Figure 1: The EFOV test on an Octopus 900 perimeter.

The EFOV test is implemented as an add-on to the Octopus control software. In contrast to usual perimetric examinations, where the subjects' head and eyes are fixated, during the assessment of EFOV the subject is allowed to move his eyes towards the presented stimulus and fixate it. A stimulus is considered as perceived if it is fixated by the subject. Therefore, no explicit subject's response (e.g. by pressing a button) is needed. The examination procedure consists of the following steps:

- Similar to conventional perimetric examinations, first the examination set-up is configured. This includes the choice of the grid of stimuli that will be presented sequentially, as well as an initial parameter setting, e.g. the definition of a time windows defining the stimulus presentation time or for capturing the user's response.
- After the general configuration of the examination, a calibration routine is started. During calibration, a mapping between the eye position in the camera image and the gaze position in the scene, i.e. on the perimeter surface, is calculated. The algorithms involved in this examination step will be discussed in the next section.
- Once the calibration procedure is successful, the examination can start. A grid of stimuli is loaded and the stimuli are presented sequentially in random order. For each stimulus the subject is encouraged to perform eye movements towards the stimulus location in order to fixate the target. The software captures the visual search behavior of the subject and the fixation (if any occurred).
- Finally, the testing results are visualized.

Figure 2 depicts the main components of the software: a communication component that encapsulates several routines for real-time communication with the Octopus perimeter hardware and software, an easy to use GUI for the examination control, several algorithms for the detection of the pupil, for calibration and gaze mapping, and a collection of routines for reading, writing and visualization purposes. The software is developed in C++ and uses the Microsoft Foundation Classes [1] (MFC).

Graphical User Interface: The graphical user interface of EFOV is simple, intuitive and aggregates following information:

- Video signal from the cupola perimeter, Figure 3 left upper part. The result of the pupil detection is denoted by a red circle. This image can be used both for fixation control and for online validation of the result of the pupil detection algorithms.
- Both presented stimulus and gaze position of the subject are visualized in a polar coordinate grid, Figure 3 right upper part. The depicted red line visualizes the eye position over the last 5 seconds.
- The graph at the bottom part of the GUI depicts the pupil size during the examination. When no pupil is found, e.g. due to blinks, the pupil size is zero. This is represented by lows in the chart. So far, the pupillographic information in only used

[1] http://msdn.microsoft.com/de-de/library/d06h2x6e.aspx

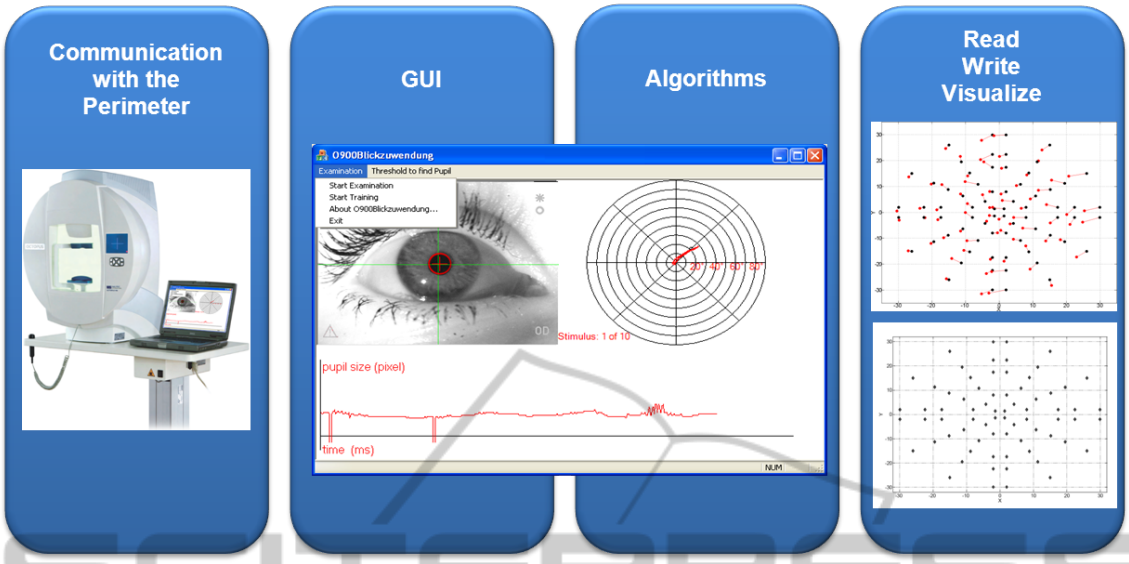

Figure 2: Components of the EFOV software.

for monitoring the eye position. In the future we will use this information to monitor the vigilance of the subjects during testing.

Furthermore the GUI provides several possibilities to configure an examination, e.g. subject data, the set-up of the stimulus grid, the size and duration of the stimuli or the response time window.

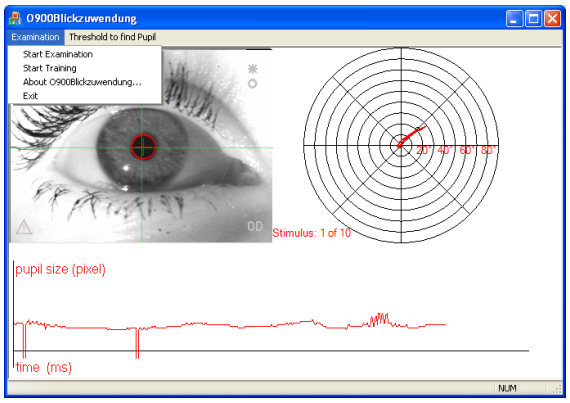

Figure 3: The Graphical User Interface of EFOV. The left upper part depicts the video signal from the cupola perimeter with the detected pupil (red circle). The presented stimulus (black circle) and the gaze position of the subject over the last 5 seconds are presented in a polar coordinate system at the right upper part. The graph at the bottom depicts the pupil size during the examination.

Read/Write and Visualization. A visualization example of EFOV testing is presented in Figure 4(b). The black dots indicate the presented stimuli (here the stimuli grid consists of 72 stimuli locations in a polar arrangement within the central 30° field of view). The red dots represent the location of the subject's fixations. Note that when a stimulus is presented, the subject is asked to search for the presented stimulus and then fixate it. The presented stimulus (black dot) and its corresponding fixation point (red dot) are connected by a red line. The longer the line, the greater is the mismatch between presented stimulus and location of the subject's fixation. Thus the length of the line represents both the exploration quality and indicates an overshoot or undershoot of the exploratory saccade.

2.1 Algorithms

To be able to detect a fixation during a video sequence, first the gaze position of the subject at each time step, i.e. video frame, has to be determined. The gaze position is the position of the pupil midpoint in the scene, i.e. cupola surface. For the detection of the pupil and gaze position we perform image processing of the video signal captured by the camera interface in the Octopus perimeters. Furthermore, changes of pupil size are monitored.

Pupil Detection. Real-time performance is a major prerequisite to the image processing algorithms. We use both global and local image features to extract the pupil. The basic idea behind it is simple: since the pupil represents an extended circular object with dark pixels, we have to search for and find such pixel groups. First, global image properties, such as the average image brightness b_{avg}, are calculated. Then, for performance reasons, every second pixel is processed. Its gray level value is compared to a threshold gray

level th that varies with the average image brightness. This threshold is defined as

$$th = \alpha * b_{avg}$$

The variable α is set empirically and can be adjusted by the user until the pupil detection is satisfactory. Since other regions in the image, such as eye lashes, may also contain dark pixel groups, for each detected group of dark pixels, it is necessary to calculate the brightness of its neighboring pixels. Only those pixels that are surrounded by dark pixels within a user-defined neighborhood area will be considered as candidates for the pupil. The pixel group that corresponds to the pupil is found by shape matching as the pixels corresponding to the pupil should form a circular object. Finally, for the identified pupil region, the area and radius is calculated. We track the position of the pupil center, which moves linearly with the direction of gaze.

Gaze Mapping and Fixation Detection. To be able to calculate the gaze position in the scene (i.e. on perimeter surface), we need to provide a mapping between the position of the eye within the camera image and the coordinates on the perimeter surface. The coordinates of the eye position are defined by the coordinates of the pupil center. The mapping is calculated during a calibration routine, as usual in eye-tracking applications. We use a 3×3 calibration grid as presented by (Li et al., 2005).

The scene points $\vec{s}_i = (x_{s_i}, y_{s_i})$ are given in polar coordinates and can be configured at the beginning of an examination. We define following default values for the coordinates $x_{s_i}, y_{s_i} \in \{-20, 0, 20\}$. The resulting nine points from the combination of these coordinates are presented during the calibration routine sequentially, where each point is presented for 5 seconds (corresponding to 100 frames at the sampling frequency of the camera). The subject is asked to fixate each presented calibration point. During stimulus presentation the eye position $\vec{e}_i = (x_{e_i}, y_{e_i})$ in the image is calculated using the algorithms for the pupil detection described above. When the eye position is stable for a time period f_T, a fixation is assumed. In order to achieve best mapping precision, during the calibration procedure we expect long fixations $f_T > 1000ms$ (corresponding to 20 video frames). Thus, the standard deviation f_D of the eye position in the image data is computed for the last 20 frames. When the standard deviation respects an empirically determined threshold $th_D = 4px$ that considers the inaccuracy of the eye tracker, $f_D < th_D$ a fixation is assumed. If a fixation cannot be recognized (e.g. due to an impaired cooperation) the missed stimulus is presented again.

The mapping of the eye position in the image to the gaze position in the scene, - perimeter surface - we use a first-order linear mapping (Li et al., 2005). For each correspondence between $\vec{s}_i$ and $\vec{e}_i$, two equations are generated that constrain the following mapping:

$$\begin{aligned} x_{s_i} &= a_{x_0} + a_{x_1} x_{e_i} + a_{x_2} y_{e_i} \\ y_{s_i} &= a_{y_0} + a_{y_1} x_{e_i} + a_{y_2} y_{e_i} \end{aligned}$$

where a_{x_i} and a_{y_i} are undetermined coefficients of the linear mapping. This linear formulation results in six coefficients that need to be determined. Given the nine point correspondences from the calibration and the resulting 18 constraint equations, the coefficients can be solved using Single Value Decomposition (Hartley and Zisserman, 2000).

In a further step, for each presented stimulus during the EFOV test, we have to find out whether the stimulus was fixated by the subject. Generally, when a presented stimulus is fixated, the subject's gaze oscillates around the stimulus location forming a fixation cluster. A fixation is assumed if the gaze is kept around the stimulus location for at least 300 ms (Liversedge et al., 2011). At a sampling rate of 20 Hz, as it is the case in the built-in cameras of the Octopus perimeter, 300ms correspond to 6 frames (or gaze points). After the presentation of a stimulus, our algorithm searches for clusters of points in at least 6 sequential video frame. This parameter is configurable and can easily be adapted to other sampling rates. If a fixation cluster is detected, we calculate the cluster centroid that represents the location of the fixation. As described above, for each stimulus location (Figure 4(b) black dots) we calculate the corresponding fixation location (Figure 4(b) red dots).

2.2 Modeling Fixation Data with the Generalized Pareto Distribution

We observed that an exact match between the location of the presented stimulus and the corresponding fixation is given very rarely. Instead, for a given stimulus location, the distribution of the distances between the stimulus location and the fixations of different subjects corresponds to a Pareto distribution. The question is: up to which distance between fixation and stimulus d_{seen} can a stimulus be considered as perceived (seen)?

We used the Generalized Pareto Distribution (GPD) to model the distribution of distances between fixation and stimulus and implemented the model using Matlab (MATLAB, 2012). The probability density function of GPD is given by the following Equation 1 (Kotz and Nadarajah, 2000), (Embrechts et al.,

1997):

$$y = f(d|k,\sigma,\theta) = (\frac{1}{\sigma})(1+k\frac{(d-\theta)}{\sigma})^{-1-\frac{1}{k}} \quad (1)$$

where d is the distance between stimulus location and fixation location, $k \neq 0$ is the shape parameter, σ the scale parameter and θ the threshold parameter. The threshold value d_{seen} was obtained from the 95% quantile of fixations of healthy (control) subjects, see Section 3.

3 RESULTS

EFOV was validated in a pilot study with 80 subjects, 40 patients with binocular visual field defects and 40 ophthalmologically healthy (control) subjects. The aim of the study was to investigate the prediction capability of EFOV for everyday living conspicuous objects within the central 30° of the visual field. Furthermore, the driving performance of the subjects was assessed in an on-road study using a dual-brake vehicle. The scope of the study was much broader and involved the investigation of visual scanning behavior and its impact on the driving performance. The ophthalmological interpretation of the results of the study is beyond the scope of this paper and will be presented in a separate article. In the following we will focus on some exemplary results of the assessment of the extended field of view to show the viability of the software.

To determine the threshold d_{seen}, i.e. the maximal distance between a perceived stimulus and the corresponding fixation, we fitted the GPD model presented in Equation 1 to the fixation data collected from the control subjects. From the 95% quantile we obtained the threshold value $d_{seen} = 10$. Thus, a stimulus is considered as perceived, if the distance between its location and the location of the corresponding fixation does not exceed 10°.

Figure 4(a) shows the binocular visual field of a subject with a homonymous visual field defect that was tested with semi-automated kinetic perimetry. The red line represents the boundary of the intact visual field. This subject is suffering from right-sided hemianopsia, therefore he has no perception within the right hemifield. Based on this result, the subject was banned from driving. Figure 4(b) depicts the EFOV testing result. The gray area represents the visual field defect from 4(a). The black dots represent the locations of the presented stimuli, while the locations of the fixation clusters are represented by red dots. As mentioned above, the location of a stimulus and its corresponding fixation are connected by a

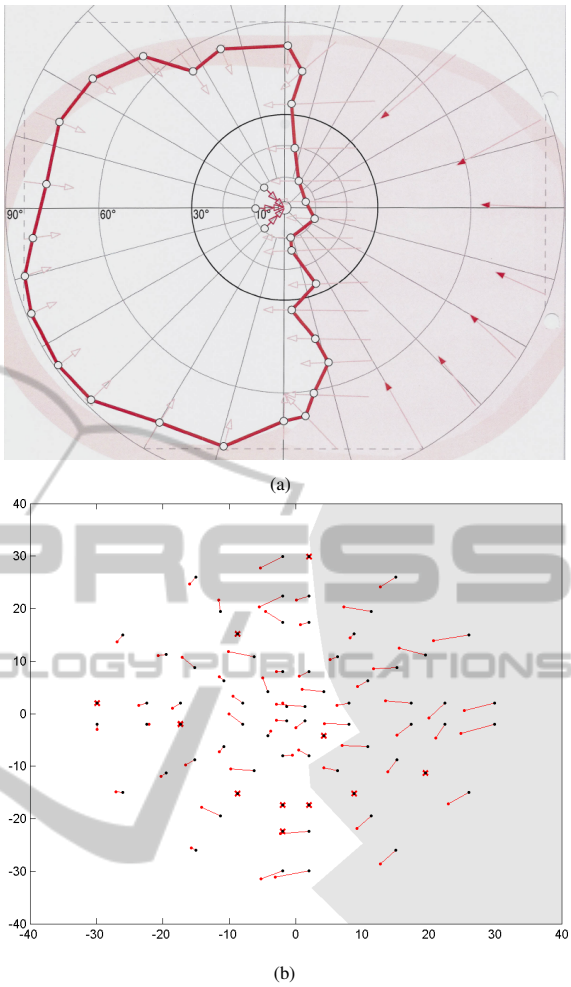

Figure 4: The performance of a subject with good exploration capability. The upper figure shows the result of a standard semi-automated kinetic perimetric examination, where the red line represents the boundary of the intact visual field. The subject can perceive only stimuli that are presented within the left hemifield. The lower figure shows the result of the exploratory field of view testing. The black dots represent the locations of the presented stimuli. The red dots are the locations of the subject's fixation. When eye movements are allowed, this subject can obviously compensate for his visual field defect.

red line. Implicitly, the line length represents the exploration capability of a subject. The longer the line, the greater is the mismatch between presented stimulus and fixation location. If the distance between the location of a presented stimulus and the location of the fixation exceeds 10°, the stimulus is considered as not seen. Such 'failed-to-see' stimuli and missing fixations (i.e. when no fixation was detected within a given response time window) are represented by red crosses. As we can see from the distances between the stimuli locations and the locations of the

fixations clusters, this patient has developed a good visual search strategy that enables him to compensate for his visual field defect.

Another example for a successful visual search strategy is shown in Figure 5. This subject can fully compensate for his visual field defect and is able to perceive all stimuli presented in the area of his visual field defect. Interestingly, both subjects passed the on-road driving assessment.

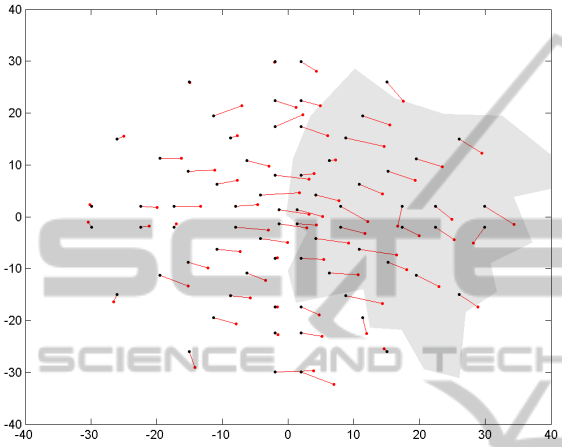

Figure 5: The EFOV result of a subject with a successful visual search strategy.

Figure 6(a) presents the visual field of another subject suffering from left sided homonymous hemianopsia. The lengths of the mismatch lines within the right hemifield and the missed stimuli indicate poor exploration capability. This subject failed the on-road driving task.

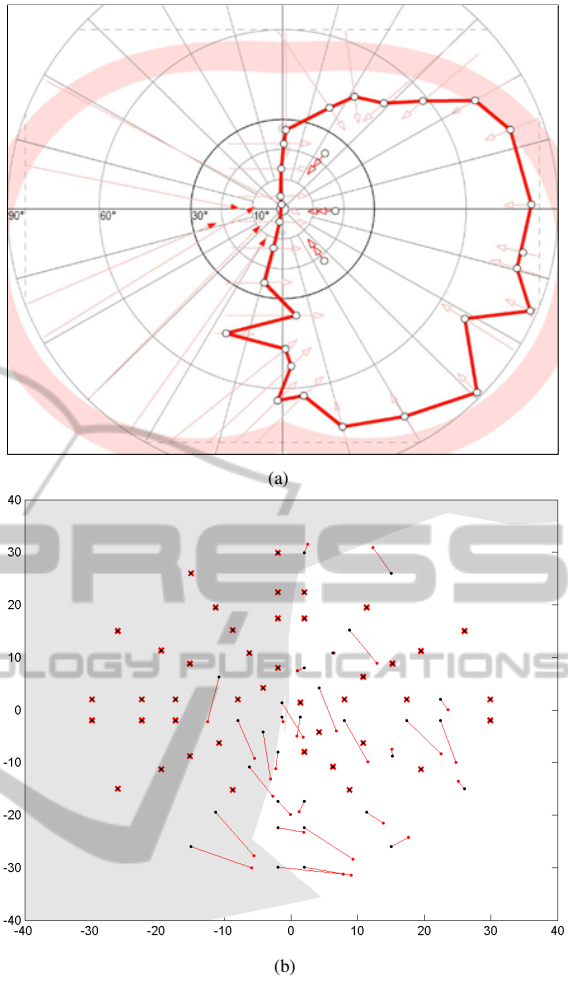

Figure 6: The performance of a subject with left sided hemianopsia. The upper figure shows the result of a standard semi-automated kinetic perimetric examination. The lower figure shows the result of the EFOV assessment. In contrast to the results of the subjects in Figures 4(b) and 5, this subject could perceive only few of the stimuli within the visual defect area. This indicates poor exploration capability.

4 CONCLUSIONS

In this paper we have presented a software for the assessment of the exploratory field of view using a conventional cupola perimeter. Pilot studies conducted so far have shown that this approach allows the assessment of exploratory capabilities, which may be more relevant than the extent and location of the visual field defect. In contrast to standard perimetric examinations, the assessment of EFOV promises to reveal the the real impact of visual field defects on activities of daily living, such as driving. Yet, broader evaluation of the method is needed.

Due to its modular structure, the EFOV software can easily be extended by further modules. Our future work will be threefold. As many subjects report loss of vigilance during visual field examinations, leading thus to an increase in the frequency of missed targets, we will develop a module for the monitoring of vigilance by using the pupillographic information (Henson and Emuh, 2010). Furthermore we plan the improvement of the calculation of fixation clusters using a Bayesian online clustering method (Tafaj et al., 2012). Up to now EFOV was developed for usage with Octopus perimeters. To make it available for a broader set of applications, we plan to integrate the testing method with existing vision analysis tools, such as Vishnoo (Tafaj et al., 2011).

REFERENCES

Embrechts, P., Klüppelberg, C., and Mikosch, T. (1997). *Modelling Extremal Events for Insurance and Finance*. Springer.

Hardiess, G., Papageorgiou, E., Schiefer, U., and Mallot, H. A. (2010). Functional compensation of visual field deficits in hemianopic patients under the influence of different task demands. *Vision Res*, 50(12):1158–1172.

Hartley, R. and Zisserman, A. (2000). *Multiple view geometry in computer vision*. Cambridge University Press, Cambridge, UK.

Henson, D. and Emuh, T. (2010). Monitoring vigilance during perimetry by using pupillography. *Invest Ophthalmol Vis Sci*, 51(7):3540–3543.

Kotz, S. and Nadarajah, S. (2000). *Extreme Value Distributions: Theory and Applications*. Imperial College Press, 1st edition.

Li, D., Winfield, D., and Parkhurst, D. J. (2005). Starburst: A hybrid algorithm for video-based eye tracking combining feature-based and model-based approaches. In *Proceedings of the 2005 IEEE Computer Society Conference on Computer Vision and Pattern Recognition (CVPR'05)*, pages 1–8.

Liversedge, S., Gilchrist, I. D., and Everling, S. (2011). *The Oxford Handbook of Eye Movements*. Oxford University Press.

Martin, T., Riley, M., Kelly, K. N., Hayhoe, M., and Huxlin, K. R. (2007). Visually guided behavior of homonymous hemianopes in a naturalistic task. *Vision Res*, 47:3434–3446.

MATLAB (2012). *version 7.14.0.739 (R2012a)*. The MathWorks Inc., Natick, Massachusetts.

Pambakian, A. L., Wooding, D. S., Patel, N., Morland, A. B., Kennard, C., and Mannan, S. K. (2000). Scanning the visual world: a study of patients with homonymous hemianopia. *J Neurol Neurosurg Psychiatry*, 69:751–759.

Riley, M., Kelly, K. N., Martin, T., Hayhoe, M., and Huxlin, K. R. (2007). Homonymous hemianopia alters distribution of visual fixations in 3-dimensional visual environments. *J Vision*, 7:289.

Schiefer, U., Wilhelm, H., and Hart, W. (2008). *Clinical Neuro-Ophthalmology: A Practical Guide*. Springer Verlag.

Tafaj, E., Kasneci, G., Rosenstiel, W., and Bogdan, M. (2012). Bayesian online clustering of eye movement data. In *Proceedings of the Symposium on Eye Tracking Research and Applications*, ETRA '12, pages 285–288, New York, NY, USA. ACM.

Tafaj, E., Kübler, T., Peter, J., Schiefer, U., Bogdan, M., and Rosenstiel, W. (2011). Vishnoo - An Open-Source Software for Vision Research. In *Proceedings of the* 24^{th} *IEEE International Symposium on Computer-Based Medical Systems*, pages 1–6.

Taylor, J. F. (1982). Vision and driving. *Practitioner*, 226:885–889.